Interface and bulk effects in the attenuation of low-energy electrons through CaF_2 thin films

J. E. Ortega
Departamento de Física Aplicada I and Departamento de Física de Materiales, Universidad del País Vasco, E-20009 San Sebastián, Spain

F. J. García de Abajo
Departamento de Ciencias de la Computación e Inteligencia Artificial, Universidad del País Vasco, San Sebastián, Spain

P. M. Echenique
Departamento de Física de Materiales, Universidad del País Vasco, San Sebastián, Spain

I. Manke, T. Kalka, and M. Dähne
Institut für Festkörperphysik der TU Berlin, Hardenbergstrasse 36, D-10623 Berlin, Germany

D. Ochs
Physikalisches Institut der TU Clausthal, Leibnizstrasse 4, D-38678 Clausthal-Zellerfeld, Germany

S. L. Molodtsov
Institut für Oberflächen und Mikrostrukturphysik, TU Dresden, Mommsenstrasse 13, D-01062 Dresden, Germany

A. Rubio
Departamento de Física Teórica, Universidad de Valladolid, E-47011 Valladolid, Spain

(Received 23 December 1997)

We have studied for low kinetic electron energies the attenuation of the Si $2p$ core-level photoemission line through epitaxial CaF_2 layers deposited on Si(111). Using an exponential attenuation model we have separated bulk and interface effects, which are, respectively, comprised within energy-dependent bulk attenuation length and interface transmission probability. The attenuation length has basically a constant value of $\sim$ 23 Å for kinetic energies above $\sim E_F+15$ eV, whereas the transmission probability has a maximum at $\sim$ 23 eV above E_F. The latter effect is consistent with the presence of a large density of bulk Λ_1 states in the conduction band of CaF_2 around 23.5 eV. Such a large density of states is obtained in a band calculation using the local-density approximation, and it is also detected in the background of secondaries of the photoemission spectra. [S0163-1829(98)01827-X]

INTRODUCTION

Large-gap insulators have many different potential applications in semiconductor technology, especially when used as epitaxial films in insulator/semiconductor or metal/insulator/semiconductor systems for hot-electron devices.[1] For this purpose, CaF_2 ($E_{gap}=12.1$ eV) is a prime candidate for a replacement of SiO_2 in metal-oxide-semiconductor (MOS) technology, due to its excellent lattice matching to silicon, with only 0.6% mismatch at room temperature. Indeed, the CaF_2/Si(111) interface attracted considerable interest in the past and now it can be considered as a well-controlled semiconductor/insulator system.

In this paper we concentrate on the scattering of electrons injected from the Si(111) substrate into the CaF_2 layer at energies around the electron-electron inelastic scattering threshold, i.e., $E_{exciton}=11.2$ eV above the conduction-band minimum (CBM).[2] This is obviously very important for a better understanding of the transport properties in this system. In this work we analyze the attenuation of low kinetic energy electrons while traversing a CaF_2 layer. These electrons are excited from Si $2p$ states by means of core-level photoemission with synchrotron radiation. In this way the Si $2p$ core-level signal is measured as a function of the film thickness and kinetic energy, the latter varied within a certain range by tuning the photon energy. Using a simple exponential attenuation model and comparing data for different thicknesses, we are able to separate bulk and interface effects in the attenuation of the Si $2p$ signal. This allows to extract the effective CaF_2 bulk attenuation length and the transmission probability across the CaF_2/Si(111) interface.

EXPERIMENT

Measurements were performed at the HE-PGM II beamline at BESSY (Berlin), using a CLAM-I spectrometer. The photon energy was varied from 107 eV to 132 eV in order to scan the photoelectron (Si $2p$) kinetic energy from $\sim$ 6 eV to 31 eV with respect to the CBM of CaF_2, which is located at 3.3 eV above the (measured) bulk Fermi level.[3] A schematic picture of the bulk energy bands for the CaF_2/Si(111) system is shown in Fig. 1. The experiments were done under normal emission geometry with a relatively large (estimated

 © 1998 The American Physical Society

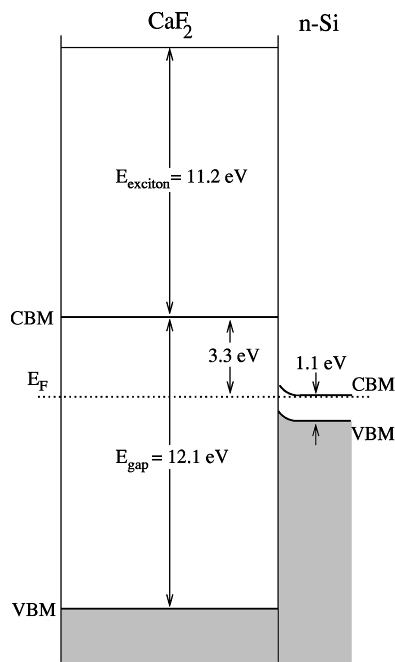

FIG. 1. Schematic plot for the relative positions of the bulk CaF_2 and n-type Si bands gaps. The e^--e^- inelastic scattering threshold is also indicated by the exciton energy (Ref. 2). Shaded areas correspond to occupied states. VBM stands for valence-band maximum.

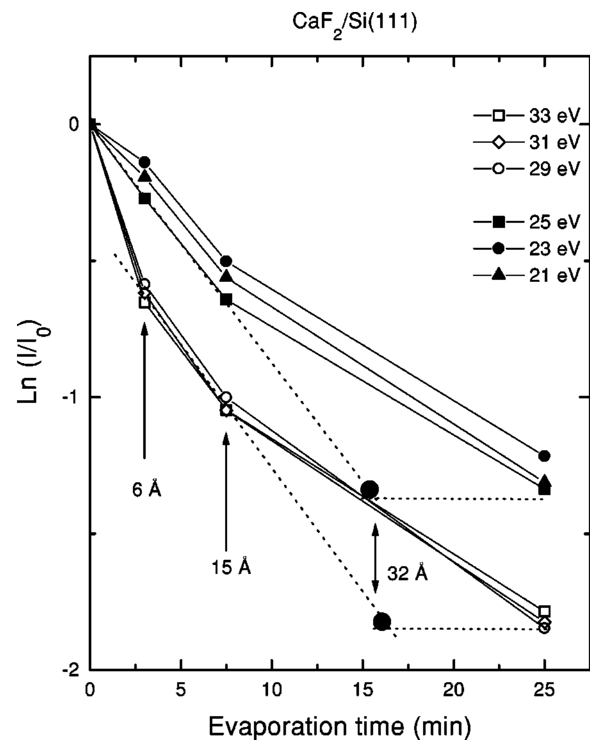

FIG. 2. Variation of the relative intensity of the Si $2p$ (total area under the peak) as a function of the CaF_2 evaporation time, at the indicated kinetic energies above E_F. The dashed, inclined lines are linear extrapolations to the data points for low exposures, whereas the horizontal line adjusts the data for 25 min to fit the linear behavior.

to be $\sim\pm10°$) acceptance angle due to the sample bias of -15 eV. The average resolution is $\sim$ 0.5 eV. n-type Si(111) wafers with ρ=10–20 Ω cm were outgassed at temperatures of 600 ° C for 12 h, subsequently annealed to 1100 °C, and then cooled down slowly for the preparation of the 7×7 surface.

FILM PREPARATION

CaF_2 films were evaporated from a water-cooled Knudsen cell on top of the Si(111) crystal held at 700 °C with a deposition rate of $\sim$2 Å min^{-1}. Such a high-temperature deposition is known to produce flat films oriented along the (111) direction, with a low density of bulk and surface defects.[4] For our purposes, it is also important to determine the correct thickness and the mode of growth of the CaF_2 film. On one hand, with the growth temperature used here there is no appreciable reevaporation of the deposited CaF_2 at least for coverages up to about 15 Å.[5,6] Thus the film thickness can be calibrated using a quartz microbalance. On the other hand, with a very low deposition rate and a high substrate temperature we expect an incomplete wetting of the substrate, with large substrate areas not being covered.[7] However, we must note that the growth parameters, like the temperature, appear to be critical in this system, and we must take care about making direct extrapolations of these parameters since important differences have been observed for nominally the same growth conditions. In that sense, using the same Si substrate, temperature calibration, and similar deposition parameters (4 Å min^{-1} and 750 °C) our scanning tunneling microscopy (STM) pictures display uniform CaF_2 films with monolayer height steps that cover the whole surface.[3] Although we do not discard the presence of a few uncovered terraces, as expected from these growth conditions,[7] the STM images show that the mode of growth of our CaF_2 films deviates very little from the ideal layer by layer, at least up to 15 Å. In Fig. 2 we show the logarithmic intensity variation of the Si $2p$ emission as a function of the evaporation time, measured at different photon energies. First we can observe a different attenuation between 0 min and 3 min for the two photon energy ranges shown. Such a behavior is due to kinetic-energy-dependent interfacial transmission effects, as we will discuss below. On the other hand, for evaporation times between 7.5 min and 25 min there is a slower attenuation of the signal that is observed with all the photon energies. Such an effect could be either due to an increasing roughness of the growing film or to a partial reevaporation of the CaF_2. An estimate of the ‘‘effective’’ thickness is obtained by extrapolating the exponential attenuation between 6 Å and 15 Å, as indicated by the dashed lines. We derive an effective coverage of $\sim$32 Å for the longer evaporation time used here.

ATTENUATION OF THE Si $2p$ LINES

In Fig. 3 we show the Si $2p$ core-level peak measured for different photon energies and the three different thicknesses of the CaF_2 overlayer. The core-level peaks are displayed after subtraction of the background of secondaries, which is obtained from spectra recorded at different photon energies, i.e, without the Si $2p$ peak in the kinetic energy region of interest. The absolute area under the peaks of Fig. 3 is plotted in Fig. 4. The almost featureless curve for clean Si(111)

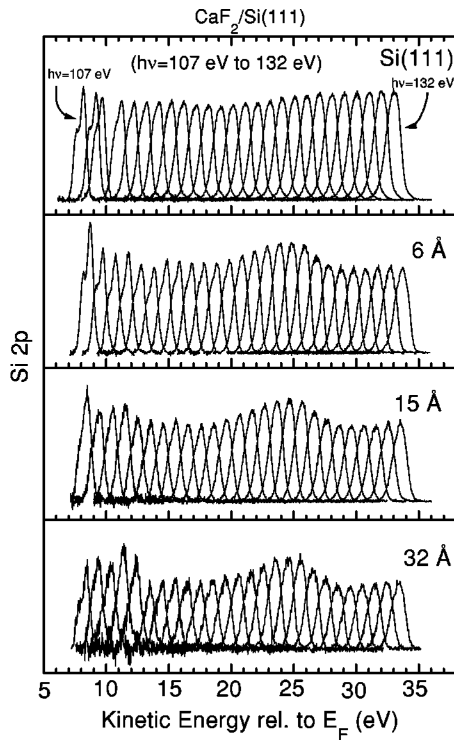

FIG. 3. Si $2p$ core-level spectra measured at low kinetic energies from a Si(111) substrate covered with epitaxial CaF_2 layers of different thicknesses. The secondary electron background has been removed.

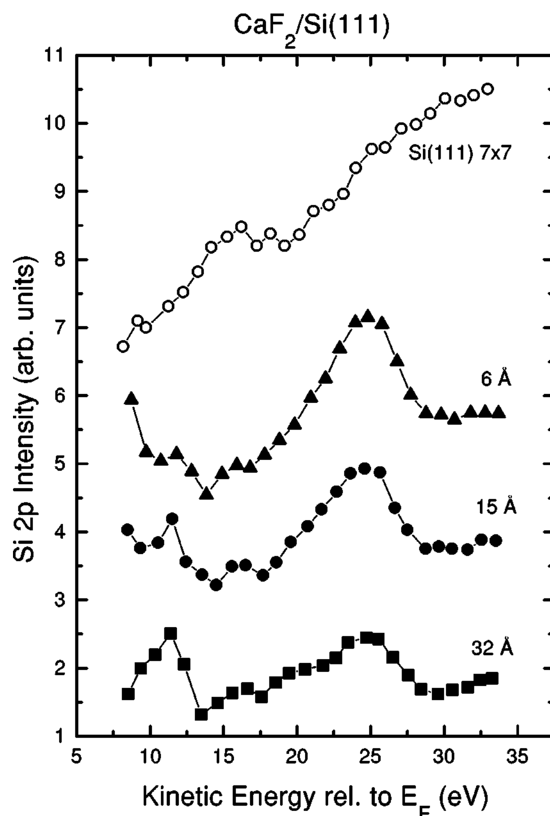

FIG. 4. Intensity of the Si $2p$ peaks shown in Fig. 3, i.e., total area under the peaks.

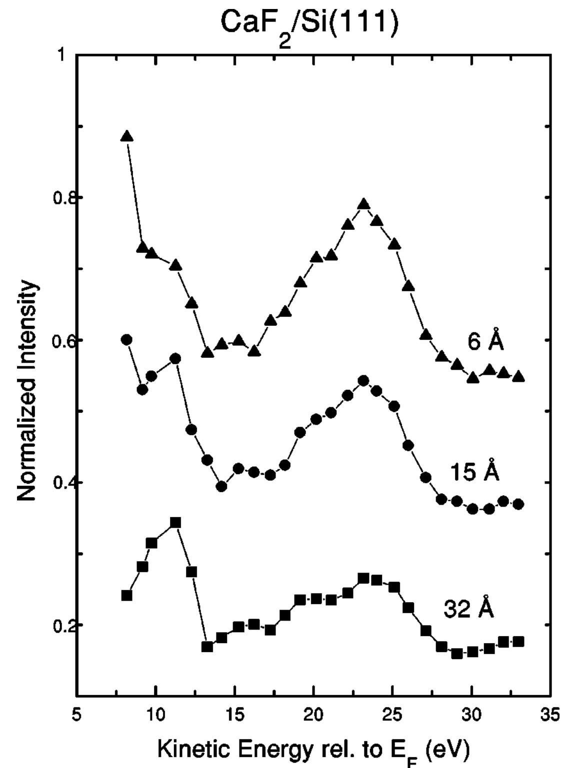

FIG. 5. Normalized intensity of the Si $2p$ peak. The Si $2p$ signal from the bare substrate in Fig. 4 has been used as a normalizing curve.

contrasts with the intensity variations for CaF_2, already observed for the thinnest film. The absolute attenuation effect of the CaF_2 overlayer can be observed in Fig. 5, where we have plotted the intensity ratio to the bare Si(111). By normalizing we also remove photon-dependent features, such as intensity variations of the incoming light and photoionization cross-section effects. We note that after normalization the curves still look similar in Figs. 4 and 5. For the 6-Å-thick film, the core level appears less attenuated at very low energy and around 23 eV, where a peak is observed. For the thickest film (32 Å) we observe a new peak emerging at ~11 eV, whereas the 23-eV feature is still visible. We can assign interface and bulk ''character'' to these two features from their qualitative thickness dependence in Figs. 4 or 5. The peak around 23 eV is an interface and/or surface effect, since its relative intensity with respect to the ''background'' remains almost constant. For instance, the relative (peak-to-valley) intensity measured at 23 eV and 29 eV stays constant at about ~1.4 for all coverages. On the other hand, the peak emerging at 11 eV is clearly a bulk effect, since it grows with coverage in comparison to the rest of the curve.

DISCUSSION

It should be noted that the two qualitative conclusions derived from Figs. 4 and 5 are made without assuming any attenuation model for electrons traversing the CaF_2 layer. However a model is needed to obtain quantitative results. It is known that the simple exponential attenuation model is strictly valid at relatively high kinetic energies, when the inelastic scattering dominates and the elastic (or ''quasielastic'') scattering occurs basically in the forward direction. At

low energies, in contrast, one has to consider the increasing probability for almost isotropic elastic scattering. This latter leads to a random-walk trajectory of the electron, though this is not affecting the simple exponential attenuation of the photoemission signal in normal emission geometry.[8] However, the assumption of the simple exponential attenuation law is particularly not justified for very thin films, since we have to take into consideration elastic scattering of electrons back into the substrate.[9] It is obvious that such an effect will affect critically the exponential attenuation law for very different scattering rates at film and substrate. This is the case of an insulating thin film deposited on top of a semiconducting or metallic substrate when we consider electron energies very close to or below the inelastic scattering threshold of the insulator. Indeed, electrons that are backscattered into the substrate may undergo here inelastic scattering and get thermalized. Nevertheless, even in the case of both strong elastic backscattering probability and extremely low inelastic rate within the insulator, such an additional ''substrate'' scattering results in a hyperbolic, i.e., quasiexponential attenuation of the substrate signal for normal emission geometry.[9] Thus we expect minor deviations in the escape depth obtained by analyzing the substrate signal with the simple exponential attenuation model or with the more appropiate ''two-flux'' approximation, even for kinetic energies below the inelastic scattering threshold.[10,11] We can then assume that the exponential attenuation model is suitable for the data analysis, especially beyond the inelastic scattering threshold of CaF_2, at least to obtain a first estimate of an *effective* electron attenuation length. Such an effective attenuation length will include both inelastic and elastic scattering effects at low kinetic energies, and will basically reflect the inelastic scattering length for higher kinetic energies.

In the exponential attenuation model the Si $2p$ intensity from the clean and the CaF_2-covered Si(111) substrate is given, respectively, by the following expressions:

$$I_0(E)=I_{Si}(E)T_{Si}(E), \quad (1)$$

$$I_d(E)=I_{Si}(E)T_{CaF_2/Si}(E)T_{CaF_2}(E)e^{-d/\lambda^*(E)}, \quad (2)$$

where $I_{Si}(E)$ is the photoemission intensity reaching the Si(111) surface (interface) layer, $\lambda^*(E)$ the energy-dependent attenuation length in the CaF_2 film along the normal direction, d the CaF_2 film thickness, and $T_{Si}(E)$, $T_{CaF_2}(E)$, and $T_{CaF2/Si}(E)$ represent the energy dependent transmission coefficients across the Si(111) and the CaF_2(111) surfaces, and across the CaF_2/Si(111) interface, respectively. Note that these transmission coefficients account for the intensity change undergone by the photoelectron beam by just crossing the surface and the interface. Thus the attenuation of the beam due to the finite thickness of the interface is included within the exponential term in Eq. (2), i.e., the same attenuation length is assumed through all the CaF_2 layers. This is justified by the abruptness of the CaF_2/Si(111) interface, where we have a bulklike geometric and electronic environment within the CaF_2 film as soon as we cross the first Ca ''contact'' layer.[12–14] It is intuitive that we can eliminate interface and surface effects by comparing data from different thicknesses. Indeed the energy-dependent bulk attenuation length is obtained by just considering photoemission data for two different values of d,[10]

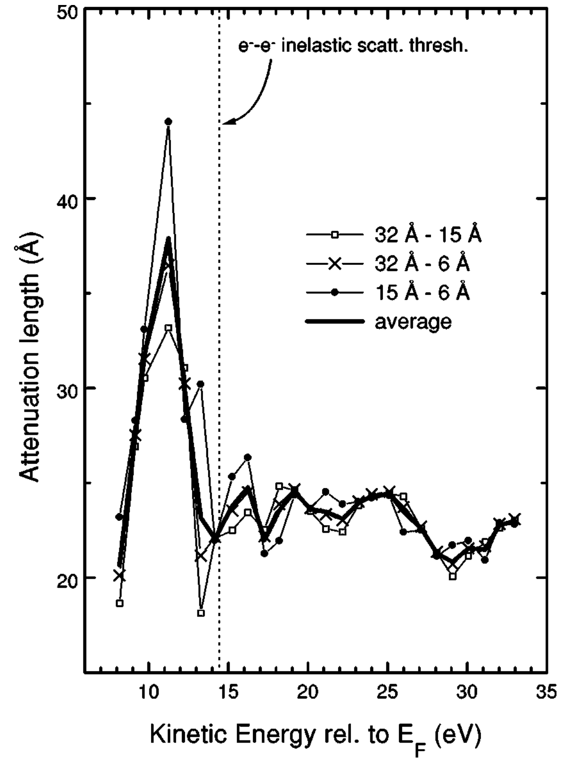

FIG. 6. Attenuation length of the photoelectron beam in CaF_2 obtained from the analysis of the data in Fig. 4 using the uniform exponential law (see the text). The symbols indicate the curves obtained for different combinations of data sets of Fig. 4.

$$\lambda^*(E)=\frac{d_2-d_1}{\ln(I_{d_1}/I_{d_2})}. \quad (3)$$

Using the data from Fig. 4 we obtain the three different attenuation-length curves plotted with symbols in Fig. 6. As we see, the three possible thickness combinations result basically in the same curve. The thick line represents an average curve. Here we note that deviations from the correct thickness in Eq. (3) lead to uncertainties in the absolute attenuation length, shifting the attenuation curve up or down, though the energy-dependent qualitative features remain unchanged. The uncertainty in the coverage ($\sim$ 20%) is thus the main error source for the absolute values obtained from Fig. 6 (for the sake of clarity we are omitting the error bars). Therefore it is not necessary to take into account minor effects, such as the fluorine monolayer (1 Å thick) sublimating to vacuum during interface formation.[12] Note that without the proper thickness calibration and correction performed in Fig. 2, we would obtain an unrealistic quantitative result in Fig. 6, i.e., a shifted curve for every thickness combination. The peak observed in Fig. 6 shows up below the inelastic scattering threshold, and it is linked to the so-called bulk feature in Fig. 5. It indicates the transition from a dominant elastic scattering at low energy to a more important inelastic scattering at a higher energy. On one hand, a strong elastic backscattering probability leads to a significant attenuation of the signal via backscattering into the substrate. Since the elastic scattering rate decreases continuously as a function of

the energy, we get an increasing attenuattion length. Around the threshold, the elastic scattering rate drops below the inelastic one, which in turn increases very quickly from this point.[10] Therefore a peak in the attenuation length is expected when the inelastic scattering takes over, i.e., around (below or above, depending on the exact scattering rates) the inelastic threshold. Beyond this point we attribute the attenuation length curve entirely to inelastic scattering.

At kinetic energies above 14.5 eV, disregarding minor features, we find the attenuation length basically constant at around 23 Å. This value is much higher than in other large-band-gap insulators, such as SiO_2, where the escape length is ~ 6–7 Å.[10] The uncertainty in the CaF_2 coverage or deviations from the ideal layer-by-layer growth cannot explain the relatively large attenuation length found in CaF_2. Thus it is a real effect that reflects a lower inelastic scattering probability. This can be due to a better crystallinity of the CaF_2 film or simply to an intrinsically lower bulk inelastic scattering rate for CaF_2. This issue is under current investigation.[15] On the other hand, we should note that by just considering the attenuation of the Si $2p$ signal (Fig. 3) at a fixed energy one gets a wrong, smaller value for the effective bulk attenuation length, since in that case interface transmission effects are not being considered. These are indeed present in our experiment, as deduced from the so-called interface feature at 23 eV in Figs. 4 and 5. In Fig. 6 such an interface feature is mostly absent, as expected.

As given in Eq. (2), the effect of the interface on the photoelectron beam is treated as a whole within the transmission probability function $[T_{CaF_2/Si}(E)]$ through the interface. From Eqs. (1) and (2) it is easy to derive the *total* transmission probability as

$$\frac{T_{CaF_2}(E)}{T_{Si}(E)} T_{CaF_2/Si}(E) = \frac{I_{d_2}}{I_0} \left(\frac{I_{d_1}}{I_{d_2}} \right)^{(d_2/d_2-d_1)}. \quad (4)$$

The electron transmission probability across both the CaF_2 and the Si(111) free surfaces should be very similar for kinetic energies well above E_F. On one hand, energy-dependent features in the emission probability from the surface are very unlikely for relatively high electron energies, since there should not be any remarkable surface density of states due to the absence of bulk band gaps. However there is a higher probability of electron emission from the CaF_2 surface due to its lower (~1.7 eV) electron affinity, though at higher kinetic energies the difference in the emission probability between both surfaces is negligible.[16] Therefore, for energies above 14.5 eV the first factor on the left-hand side of Eq. (4) is expected to be an almost flat function of the energy, very close to unity. Thus the right part is basically giving the energy dependent features of the transmission probability across the CaF_2/Si(111) interface, i.e., $T_{CaF_2/Si}(E)$. In Fig. 7 we plot the total transmission probability according to Eq. (4) for the three possible combinations of d_1 and d_2. The behavior at very low energies (dashed lines) could be related to the lower electron affinity of CaF_2(111) with respect to Si(111), as simply deduced from Eq. (4). Nevertheless we prefer to disregard this energy range due to the less applicability of the exponential attenuation model. The so-called interface feature in Figs. 4 and 5

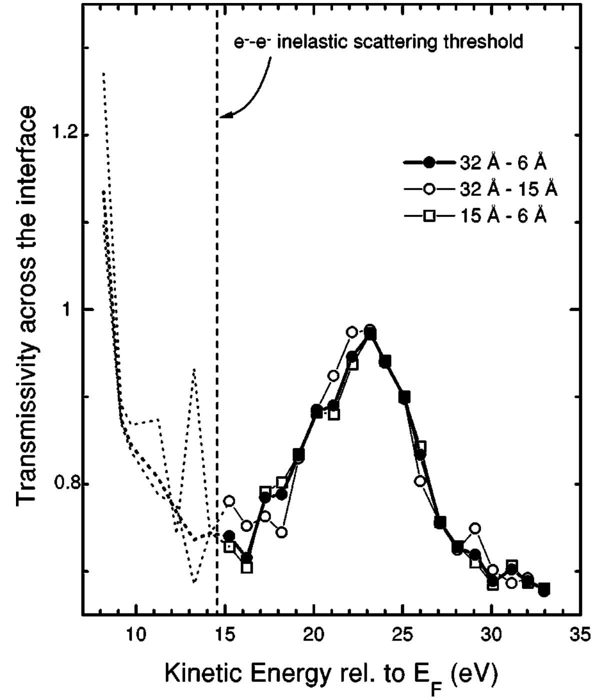

FIG. 7. Effective transmission probability across the CaF_2 interface derived using the exponential attenuation law. The dashed line indicates the result for the low-energy region, where the exponential attenuation model is less appropriate.

appears now as a *resonant transmission peak* at ~ 23 eV, which represents a 25–30 % increase in the Si $2p$ intensity. Indeed, the total transmissivity T_{int} varies from 0.72 at ~ 16 eV to 0.98 at 23 eV and back to 0.68 at 33 eV. If surface effects are negligible as discussed above, we can interpret Fig. 7 as the photoelectron beam almost completely transmitted across the interface at 23 eV while it is partially reflected or absorbed otherwise.

The bulk density of states within the film affects the photoelectron intensity as soon as the interface is crossed. Thereby the simplest explanation for the energy-dependent features in the *interface* transmission probability curve of Fig. 7 is the availability of *bulk* states within the CaF_2 film for electron transport. The peak in Fig. 7 is too sharp to be due to photoelectron diffraction effects at the interface. Moreover, due to our large acceptance angle, we expect minor photoelectron diffraction contributions. In order to analyze the influence of the bulk electronic structure of CaF_2 we have calculated its band structure using the local-density approximation (LDA). The details will be given elsewhere.[15] The band dispersion along the (111) direction, i.e., the direction perpendicular to the film, is displayed in the upper part of Fig. 8. In the lower part we show the total density of states (DOS) together with the density of Λ_1 states, which are the states along the (111) direction. The thin line is the average transmission probability curve from Fig. 7. The calculated CBM has been adjusted to the experimental one following Fig. 1. In Fig. 8 we observe how the transmission peak, which is centered at 23 eV, appears at the same energy where the DOS is maximum for Λ_1 symmetry. Note that the electron wave function in Λ_1 states has the largest projection along the (111) direction, thereby providing the most important conduction channel across the CaF_2 film. This is re-

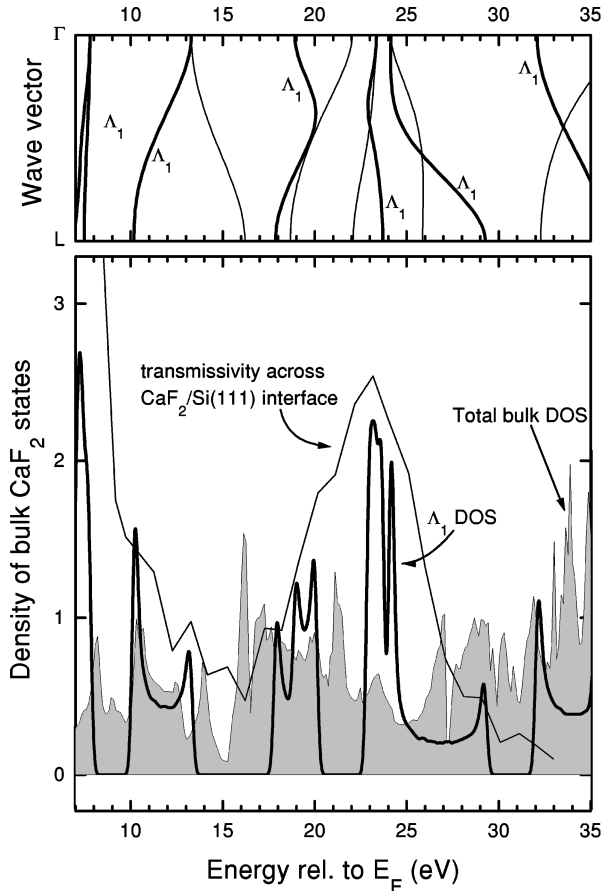

FIG. 8. Top, bulk energy bands for CaF_2 along the (111) direction. Bottom, total density of states for bulk CaF_2 (shaded, given in states/cell/eV) and density of states for Λ_1 symmetry along (111) (thick line, given in states/BZ-line/eV). The peak in the transmission probability curve of Fig. 7 (thin line) that is coincident with the high density of Λ_1 states.

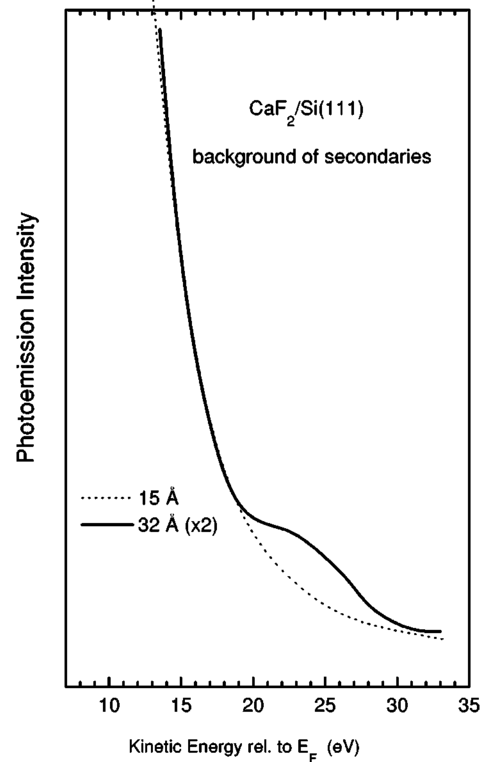

FIG. 9. Background of secondaries of the photoemission spectra for 15 Å (dashed line) and 32 Å (solid line) around 23 eV. The spectra have been taken under normal emission and hν = 130 eV. The peak is related to the CaF_2 bulk density of states of Λ_1 symmetry.

flected in the transmission curve, i.e., the presence of the very high density of Λ_1 states around 23.5 eV electrons allows the complete transmission of the photoelectrons injected from the Si(111) interface ($T=0.98$). Although other Λ_1 states seem to contribute to the transmission peak, above and below 23.5 eV, the Λ_1 gap centered around 21.5 eV is not giving rise to a corresponding decrease in the transmissivity. This is probably due to the large acceptance angle of our experiment. For the upper Λ_1 band above 32 eV there is no remarkable contribution to the electron transmission. On the other hand, we must recall that Λ_1 states are the final photoemission states under normal emission, i.e., Λ_1 states are preferently detected with our measurement geometry. Thus one might initially think that the transmission curve of Fig. 7 simply reflects the detection probability of our analyzer. However, we note that, if symmetry is preserved during transmission across the interface, the detection probability is the same in both Eqs. (1) and (2), and it cancels out in Eq. (4).

Local density-of-states extrema in the conduction band can also be detected as modulations of the background of secondaries in angle-resolved photoemission spectra. They appear at a fixed kinetic energy and, under normal emission from the (111) surface, they correspond to conduction-band states with Λ_1 symmetry. In Fig. 9 we show the spectrum of secondaries taken for 15-Å and 32-Å-thick CaF_2 layers. Both spectra were recorded with $h\nu=130$ eV, though similar results are obtained for other photon energies. When comparing the data for 15 Å and 32 Å we observe a peak emerging around 23 eV, i.e., basically coincident with the maximum DOS of Λ_1 symmetry in the band calculation of Fig. 8.[17] Thus the secondaries also reflect the high DOS that leads to the transmission peak of Fig. 7. On the other hand, these conduction-band features in the background of secondaries are typical for large gap insulators, though they are commonly observed below the e^--e^- inelastic scattering threshold.[18] This is explained as due to electrons that fill out the conduction-band states below the threshold after being scattered. Since these electrons have lost any information about initial states, the spectrum of secondaries reflects the density of final states, with a peaking intensity at local conduction-band minima.[18] In contrast, the final-state DOS peak in Fig. 9 is found above the inelastic scattering threshold for CaF_2. Thus a similar phenomenum might also be taking place in our case, i.e., an extra ''filling'' of the conduction bands beyond the threshold. This is in agreement with the large attenuation length obtained at this energy range (Fig. 6).

SUMMARY

In summary we have measured the attenuation length and the interface transmission probability for CaF_2 films around

the inelastic scattering threshold. The former is basically constant around 23 Å for energies above the inelastic scattering threshold, in contrast to the small value found for SiO_2. This result indicates a still too low inelastic scattering rate beyond the threshold, though the reason for that is not clear. The transmission probability displays a resonant peak around 23 eV, coincident with a high density of bulk CaF_2 states projected along the normal direction. Such a high density of states is detected also in the secondaries of the photoemission spectra.

ACKNOWLEDGMENTS

The authors are pleased to acknowledge Professor Kaindl for providing us with the photoemission chamber. This work has been supported by the European Community through the HCM program (HCM 68/96).

[1] L. J. Schowalter and R. W. Fathauer, Crit. Rev. Solid State Mater. Sci. **15**, 4 (1989).

[2] G. W. Rubloff, Phys. Rev. B **5**, 662 (1972).

[3] M. T. Cuberes, A. Bauer, H. J. Wen, M. Prietsch, and G. Kaindl, J. Vac. Sci. Technol. B **12**, 2646 (1994).

[4] F. J. Himpsel, U. O. Karlsson, J. F. Morar, D. Rieger, and J. A. Yarmoff, Phys. Rev. Lett. **56**, 1497 (1986).

[5] D. Rieger, F. J. Himpsel, U. O. Karlsson, F. R. McFeely, J. F. Morar, and J. A. Yarmoff, Phys. Rev. B **34**, 7295 (1986).

[6] J. D. Denlinger, E. Rotenberg, U. Hessinger, M. Leskovar, and M. A. Olmstead, Phys. Rev. B **51**, 5352 (1995).

[7] U. Hessinger, M. Leskovar, and M. A. Olmstead, Phys. Rev. Lett. **75**, 2380 (1995).

[8] W. S. M. Werner, Surf. Sci. **257**, 319 (1991).

[9] J. Bernasconi, E. Cartier, and P. Pfluger, Phys. Rev. B **38**, 12 567 (1988).

[10] F. R. McFeely, E. Cartier, J. A. Yarmoff, and S. A. Joyce, Phys. Rev. B **42**, 5191 (1990).

[11] A test for the validity of the exponential attenuation law versus the two-flux approximation, which considers the backscattering into the substrate, has been done by MacFeely *et al.* in SiO_2.[10] For kinetic energies just below the inelastic scattering threshold it is found an underestimation of the correct escape depth of less than 20% if the simple exponential attenuation model is used. For CaF_2 we expect an even smaller deviation, since the kinetic energy for the threshold is larger and the elastic scattering rate decreases considerably at this energy range. On the other hand, the two-flux approximation requires an independent determination of the elastic scattering rate to obtain the inelastic scattering contribution to the escape depth. Instead of introducing new parameters in the data analysis, we, rather, keep the simplicity of the exponential model, being aware that this model might give a ~20% deviation of the escape length for low kinetic energies.

[12] R. M. Tromp and M. C. Reuter, Phys. Rev. Lett. **61**, 1756 (1988).

[13] D. Rieger, F. J. Himpsel, U. O. Karlsson, F. R. McFeely, J. F. Morar, and J. A. Yarmoff, Phys. Rev. B **34**, 7295 (1986).

[14] C. Arcangeli, S. Ossicini, and O. Bissi, Surf. Sci. **269/270**, 743 (1992).

[15] A. Rubio *et al.* (unpublished). We are currently examining the influence of the bulk band structure of CaF_2 in the inelastic scattering, in particular, the presence of localized states in the conduction band close to the inelastic threshold [see, for instance, N. V. Smith, G. K. Wertheim, A. B. Andrews, and C.-T. Chen, Surf. Sci. Lett. **282**, L359 (1993)].

[16] A rough estimate to the transmission probability across the surface for CaF_2 and Si(111) can be obtained using a step potential for the surface barrier (see for instance E. Merzbacher, *Quantum Mechanics*, Wiley International, New York, 1970). For electron energies above 22 eV, that gives the same transmission probability across both surfaces within 3%.

[17] The peak in Fig. 9 cannot be due to the Ca MNN transition. Although this transition is found at 20 eV for metallic Ca, it should be discarded for CaF_2 since most of the Ca s electrons have been transferred to F atoms. At any rate, the relative position of the valence band in CaF_2 (see Fig. 1) and the position of the Ca $3p$ and $3s$ levels at 28.0 and 47.0 eV, respectively (see Ref. 5), set any possible Ca MVV transition at about 11 eV and 30 eV with respect to E_F, respectively.

[18] F. J. Himpsel and W. Steinmann, Phys. Rev. B **17**, 2537 (1978); D. A. Lapiano-Smith, E. A. Eklund, F. J. Himpsel, and L. Terminello, Appl. Phys. Lett. **59**, 2174 (1991); S. L. Molodtsov, A. Puschmann, C. Laubschat, G. Kaindl, and V. K. Adamchuk, Phys. Rev. B **44**, 1333 (1991).